

# Effective thermal conductivity of porous materials and composites as a function of fundamental structural parameters

Yusuke Asakuma

*Department of Mechanical and Systems Engineering, University of Hyogo  
2167 Shosha, Himeji, 671-2280, Japan  
e-mail: asakuma@eng.u-hyogo.ac.jp*

Tsuyoshi Yamamoto

*Department of Chemical Engineering, Kyushu University  
744 Motooka Nishi-ku Fukuoka 819-0395, Japan*

We conducted thermal conductivity investigations by homogenization. This method can effectively model structural features such as pores within dispersed particle architectures via a finite element mesh. We investigated the factors that determine the effective thermal conductivity of porous structures and composites, such as the volume ratio of the continuous and dispersed phases, conductivity ratio, Biot number and particle packing model.

**Keywords:** homogenization method, effective thermal conductivity, multi-scale.

## NOMENCLATURE

$Bi$	–	Biot number
$G$	–	Dimensionless heat generation number
$g$	–	Volumetric rate of heat generation
$h$	–	Interfacial thermal conductance
$L$	–	Characteristic macroscopic length
$l$	–	Characteristic microscopic length
$\mathbf{n}$	–	Unit normal to $\Gamma$
$T$	–	Temperature
$\Delta T$	–	Imposed temperature difference
$V$	–	Void fraction
$x$	–	Dimensionless macro-scale variable
$x^*$	–	Dimensional macro-scale variable
$y$	–	Dimensionless microscale variable
$\alpha$	–	Thermal conductivity ratio
$\chi$	–	Particular solution of $T$
$\delta$	–	Identity matrix
$\varepsilon$	–	Small parameter ( $l/L$ )
$\Gamma$	–	Common boundary of the two media

---

$\Lambda$	–	Dimensionless thermal conductivity
$\lambda$	–	Dimensional thermal conductivity
$\nu$	–	Weight function
$\theta$	–	Temperature
$\Omega$	–	Domain

## SUBSCRIPTS

$c$	–	Continuous phase (solid)
$d$	–	Dispersed phase (solid)
eff	–	Effective
$g$	–	Gas
$p$	–	Number of spatial dimensions
$q$	–	Number of spatial dimensions
$s$	–	Solid
0, 1, 2	–	Asymptotic expansion indices

## 1. INTRODUCTION

The porous material and composites have been used for adiabatic material and reinforcement due to the fact that they have the advantage of lower heat conduction and a high strength. However, heat conduction in the porous material and composites becomes very complicated because the parameters such as pore size, porosity and pore distribution, particle size and particle distribution are heterogeneous. The effective thermal conductivity (ETC) is very important because thermal expansion by disordered temperature distribution and temperature gradient causes stress concentration around pore and composite. The conventional models for heat transfer in porous material and composite [4, 5] are not perfectly adequate because they are simplified and treated as two-dimensional system.

Thermal and structural analyses have to be conducted simultaneously and precisely. However, there is less research that focuses on the microstructure of the porosity. Here, the homogenization method is introduced as the multi-scale analysis, which can reflect the microstructure of pore and particle on the macro property such as the thermal conductivity. This method is applied to the stress and the fracture analysis frequently [7, 9], and then it is being developed in thermal analysis [2, 3, 6, 8]. Therefore, we think that the homogenization method is very useful for the complex material because it can precisely examine the change of the microstructure after several operations and reactions under severe surroundings. We used the finite element method to investigate the mechanism of heat transfer in porous materials, which enabled calculation of the effective thermal conductivity. We investigated the effects of particle packing, porosity and Biot number on the thermal conductivity.

## 2. MODEL

As a first step in analyzing porous materials and composites, schematically shown in Fig. 1a, we considered the simple periodic composite structure shown in Fig. 1b. As shown in Fig. 1c, each cell of this periodic structure consists of two domains: solid ( $\Omega_s$ ) and gas ( $\Omega_g$ ). We defined  $\Gamma$  to be the interface between the two domains.

The periodic domain  $\Omega$  is small compared with the characteristic length  $L$  at the macroscopic scale:

$$\varepsilon = \frac{l}{L} \ll 1, \quad (1)$$

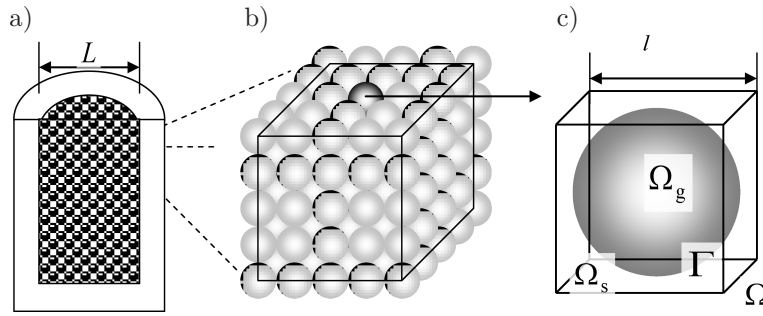


**Fig. 1.** Schematic of model used for homogenization: a) porous material, b) periodic structure, c) unit cell

where  $\varepsilon$  is a scale parameter, and  $l$  and  $L$  can be understood as the characteristic sizes of the sample at the microscopic and the macroscopic scales, respectively. In this analysis,  $l$  is the pore diameter of the porous material and  $\varepsilon$  ranges from about  $10^{-6}$  to  $10^{-4}$ .

The multi-scale periodic heat conduction problem under steady-state conditions for the medium described above can hence be mathematically expressed as

$$-\frac{\partial}{\partial x_j^*} \left( \lambda_s \frac{\partial T_s}{\partial x_j^*} \right) = g_s \quad \text{in } \Omega_s, \quad (2)$$

$$-\frac{\partial}{\partial x_j^*} \left( \lambda_g \frac{\partial T_g}{\partial x_j^*} \right) = g_g \quad \text{in } \Omega_g, \quad (3)$$

$$-\lambda_s \frac{\partial T_s}{\partial x_j^*} \mathbf{n}_j = -\lambda_g \frac{\partial T_g}{\partial x_j^*} \mathbf{n}_j \quad \text{on } \Gamma, \quad (4)$$

$$-\lambda_s \frac{\partial T_s}{\partial x_j^*} \mathbf{n}_j = h (T_s - T_g) \quad \text{on } \Gamma, \quad (5)$$

where  $\lambda$ ,  $T$  and  $g$  are the thermal conductivity, temperature field and volumetric rate of heat generation on a microscopic scale, respectively. Furthermore,  $\mathbf{n}$  is the outward-pointing unit vector locally normal to the boundary  $\Gamma$  and  $h$  is the interfacial thermal conductance. Equations (2)–(5) are general expressions, and  $g_s$  and  $g_g$  become zero in the case of porous material.

By defining the following nondimensionalized quantities:

$$y \equiv \frac{x^*}{l}, \quad \theta \equiv \frac{T}{\Delta T}, \quad \Lambda \equiv \frac{\lambda_g}{\lambda_s}, \quad (6)$$

in which  $\Delta T$  is the external temperature difference on the macroscopic scale, we can rewrite Eqs. (2)–(5) as

$$-\frac{\partial}{\partial y_j} \left( \frac{\partial \theta_s}{\partial y_j} \right) = G_s \quad \text{in } \Omega_s, \quad (7)$$

$$-\frac{\partial}{\partial y_j} \left( \Lambda \frac{\partial \theta_g}{\partial y_j} \right) = G_g \quad \text{in } \Omega_g, \quad (8)$$

$$-\frac{\partial \theta_s}{\partial y_j} \mathbf{n}_j = -\Lambda \frac{\partial \theta_g}{\partial y_j} \mathbf{n}_j \quad \text{on } \Gamma, \quad (9)$$

$$-\frac{\partial \theta_s}{\partial y_j} \mathbf{n}_j = \text{Bi} (\theta_s - \theta_g) \quad \text{on } \Gamma. \quad (10)$$

Here, the dimensionless heat generation numbers and the Biot number are given by

$$G_s \equiv g_s \frac{l^2}{\lambda_s \Delta T}, \quad G_g \equiv g_g \frac{l^2}{\lambda_g \Delta T}, \quad \text{Bi} \equiv \frac{hl}{\lambda_s}. \quad (11)$$

Multiplying Eqs. (7) and (8) by a weight function  $\nu$ , integrating over  $\Omega$  and applying Green's first identity theorem we obtain

$$\int_{\Omega_s} \frac{\partial \nu_s}{\partial y_j} \frac{\partial \theta_s}{\partial y_j} dy - \int_{\Gamma} \nu_s \frac{\partial \theta_s}{\partial y_j} \mathbf{n}_j ds = \int_{\Omega_\alpha} G_s \nu_s dy, \quad (12)$$

$$\int_{\Omega_g} \Lambda \frac{\partial \nu_g}{\partial y_j} \frac{\partial \theta_g}{\partial y_j} dy + \int_{\Gamma} \Lambda \nu_g \frac{\partial \theta_g}{\partial y_j} \mathbf{n}_j ds = \int_{\Omega_g} G_g \nu_g dy \quad (13)$$

and we substitute Eqs. (9) and (10) into Eqs. (12) and (13):

$$\int_{\Omega} \alpha \frac{\partial \nu}{\partial y_j} \frac{\partial \theta}{\partial y_j} dy - \int_{\Gamma} \text{Bi} \nu \theta ds = \int_{\Omega} G \nu dy, \quad (14)$$

where  $\alpha = 1$  if  $y \in \Omega_s$ , and  $\alpha = \Lambda$  if  $y \in \Omega_g$ .

The homogenization method is thus applied to the variational weak form of the multi-scale heat conduction problem given in Eq. (14). The method proceeds by using the nondimensionalized temperature field  $\theta(x, y)$  as a function of the two spatial variables  $x$  and  $y$ , where  $x$  is given by

$$x \equiv \frac{x^*}{L} \quad (15)$$

and we introduce the following multi-scale asymptotic expansions:

$$\theta(x, y) = \theta_0(x, y) + \varepsilon \theta_1(x, y) + \varepsilon^2 \theta_2(x, y) + \dots, \quad (16)$$

$$\nu(x, y) = \nu_0(x, y) + \varepsilon \nu_1(x, y) + \varepsilon^2 \nu_2(x, y) + \dots, \quad (17)$$

where  $\theta_k(x, y)$  and  $\nu_k(x, y)$  ( $k = 1, 2, \dots$ ) are periodic functions of  $y$  at each micro level.  $\theta_0(x, y)$  and  $\nu_0(x, y)$  is macroscopic temperature and weight function, respectively. During the computations, we must account for the fact that  $x$  and  $y$  are considered to be independent variables. To this end, the derivative operator is expressed as

$$\frac{\partial}{\partial y_j} = \frac{\partial}{\partial y_j} + \varepsilon \frac{\partial}{\partial x_j}. \quad (18)$$

The homogenization process where  $\varepsilon \rightarrow 0$  produces a set of equations satisfied by  $\theta_0$ , and represents the macroscopic behavior of the bed's heat transfer.

Substituting Eqs. (16) and (17) into Eq. (14), and applying the chain rule in Eq. (18), we obtain

$$\int_{\Omega} \alpha \left( \frac{\partial \nu_0}{\partial y_j} + \varepsilon \frac{\partial \nu_0}{\partial x_j} + \varepsilon \frac{\partial \nu_1}{\partial y_j} + \varepsilon^2 \frac{\partial \nu_1}{\partial x_j} + \varepsilon^2 \frac{\partial \nu_2}{\partial y_j} \right) \left( \frac{\partial \theta_0}{\partial y_j} + \varepsilon \frac{\partial \theta_0}{\partial x_j} + \varepsilon \frac{\partial \theta_1}{\partial y_j} + \varepsilon^2 \frac{\partial \theta_1}{\partial x_j} + \varepsilon^2 \frac{\partial \theta_2}{\partial y_j} \right) dy \\ + \int_{\Gamma} \text{Bi} (\nu_0 + \varepsilon \nu_1 + \varepsilon^2 \nu_2) (\theta_0 + \varepsilon \theta_1 + \varepsilon^2 \theta_2) ds = \int_{\Omega} G (\nu_0 + \varepsilon \nu_1 + \varepsilon^2 \nu_2) dy. \quad (19)$$

The final step of the homogenization process is to group the terms associated with each power of  $\varepsilon$ , which leads to two boundary value problems: one in the homogenized macroscopic region, and the other in each periodic cell [10]. Grouping  $\varepsilon^0$  terms, we determine that  $\theta_0$  is invariant on the

macro-scale. In addition, by assuming that  $\text{Bi} = O(\varepsilon^0)$  (i.e.,  $\varepsilon \ll \text{Bi} \ll 1/\varepsilon$ ) and that  $G = O(\varepsilon^2)$ , grouping  $\varepsilon^2$  terms gives

$$\int_{\Omega} \alpha \frac{\partial \nu_1}{\partial y_j} \left( \frac{\partial \theta_0}{\partial x_j} + \frac{\partial \theta_1}{\partial y_j} \right) dy + \int_{\Gamma} \text{Bi} \nu_1 \theta_1 ds = 0. \quad (20)$$

We next define the characteristic function  $\chi_p(y)$  of arbitrary additive  $y$  as follows:

$$\theta_1(x, y) = -\chi_p(y) \frac{\partial \theta_0(x)}{\partial x_p}. \quad (21)$$

$\chi_p(y)$  is a periodic solution of Eq. (20) and corresponds to a unit temperature gradient. Substituting Eq. (21) into Eq. (20) gives

$$\int_{\Omega} \alpha \left( \delta_{jp} - \frac{\partial \chi_p}{\partial y_j} \right) \frac{\partial \nu_1}{\partial y_j} \frac{\partial \theta_0}{\partial x_p} dy = \int_{\Gamma} \text{Bi} \nu_1 \chi_p \frac{\partial \theta_0}{\partial x_p} ds, \quad (22)$$

where  $\delta$  is Kronecker's delta, and simplifying Eq. (22) gives

$$\int_{\Omega} \alpha \frac{\partial \nu_1}{\partial y_j} \frac{\partial \chi_p}{\partial y_j} dy + \int_{\Gamma} \text{Bi} \nu_1 \chi_p ds = \int_{\Omega} \alpha \frac{\partial \nu_1}{\partial y_p} dy. \quad (23)$$

Equation (23) can then become the cell problem for the characteristic function,  $\chi_p(y)$ , which is solvable by a finite element method. Here, ETC  $\lambda_{eff}$  is obtained as the homogenized property as follows:

$$\lambda_{\text{eff},p} = \frac{1}{\Omega} \int_{\Omega} \alpha \left( \delta_{pq} - \frac{\partial \chi_q}{\partial y_p} \right) dy. \quad (24)$$

We used a  $40 \times 40 \times 40$  finite element mesh, with body-centered cubic (BCC), face-centered cubic (FCC), and simple packed (SP) models for pore arrangements, and we varied the porosity by varying the radius from the center of the pore. To characterize the effect of the surface area between the solid and gas phases, boxels of the gas phase are randomly distributed. We confirmed the validity of our model and the mesh number through a comparison with the results of Rocha et al. [1]. The Biot number, which is important for heat transfer calculations, typically depends on the diameter, distance from the surface, and shape (e.g., open or closed) of a pore. The Biot number of metal hydrides, for example, is approximately 1–100 when considering convection in a packed bed [1]. We evaluated cases in which the Biot number is 0.01, 1, and 100. The thermal conductivity ratio ( $\lambda_s/\lambda_g$ ) of a material provides valuable information with respect to temperature, pore size, and pressure measurements, and is constant (e.g.,  $1/\Lambda = \lambda_s/\lambda_g = 2, 5, 10,$  and  $20$ ) for our porous materials and composites.

### 3. RESULTS AND DISCUSSION

#### 3.1. Porous material

Figures 2–5 show the effective thermal conductivity (ETC) for each Biot number and thermal conductivity ratio ( $\lambda_s/\lambda_g = 2, 5, 10,$  and  $20$ ). When the conductivity ratio and Biot number are small, as shown in Fig. 2a, the ETC can become less than 1. Heat is conducted through only the solid phase because no heat is transferred through the solid-gas interface. When the porosity is greater than 0.6 (SP) and 0.75 (FCC and BCC), heat is transferred through the gas phase

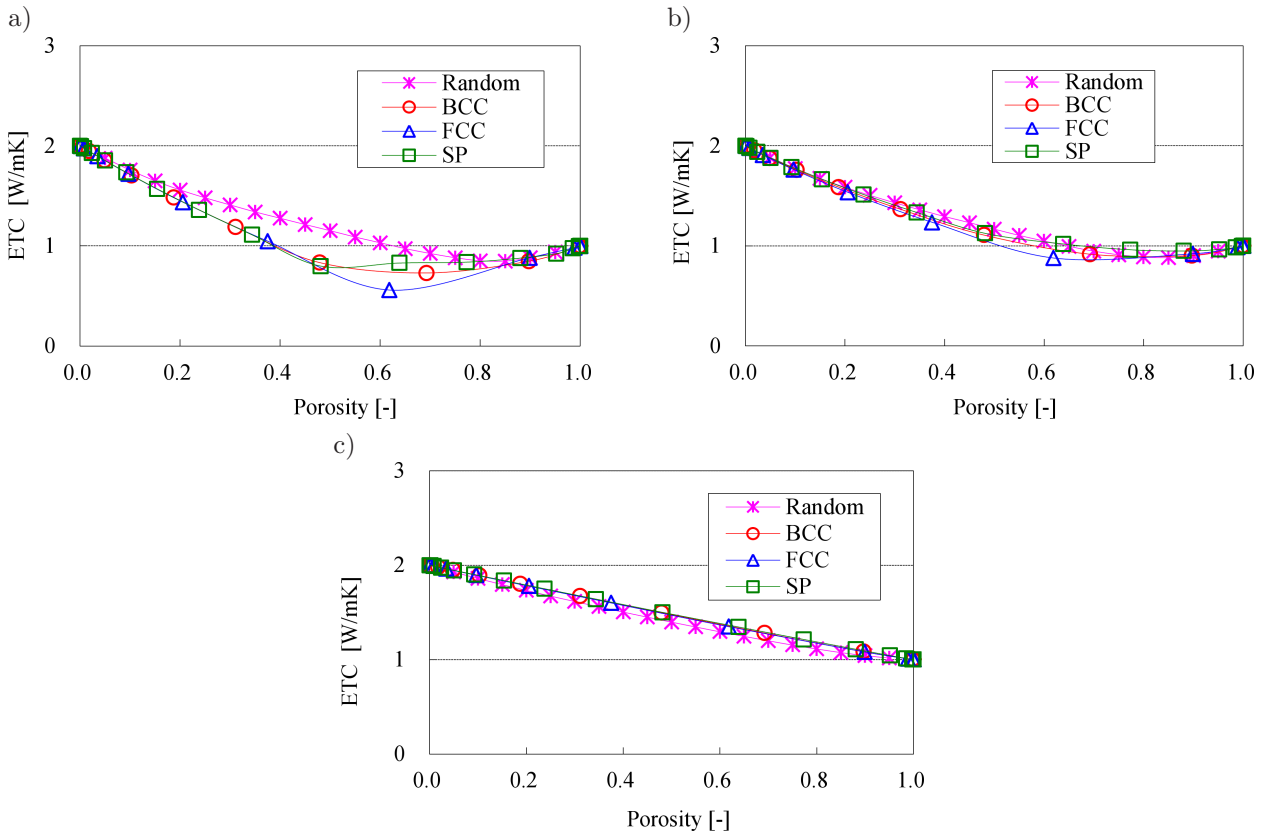


Fig. 2. ETC versus porosity for  $\lambda_s/\lambda_g = 2$ : a)  $Bi = 0.001$ , b)  $Bi = 1$ , c)  $Bi = 100$ .

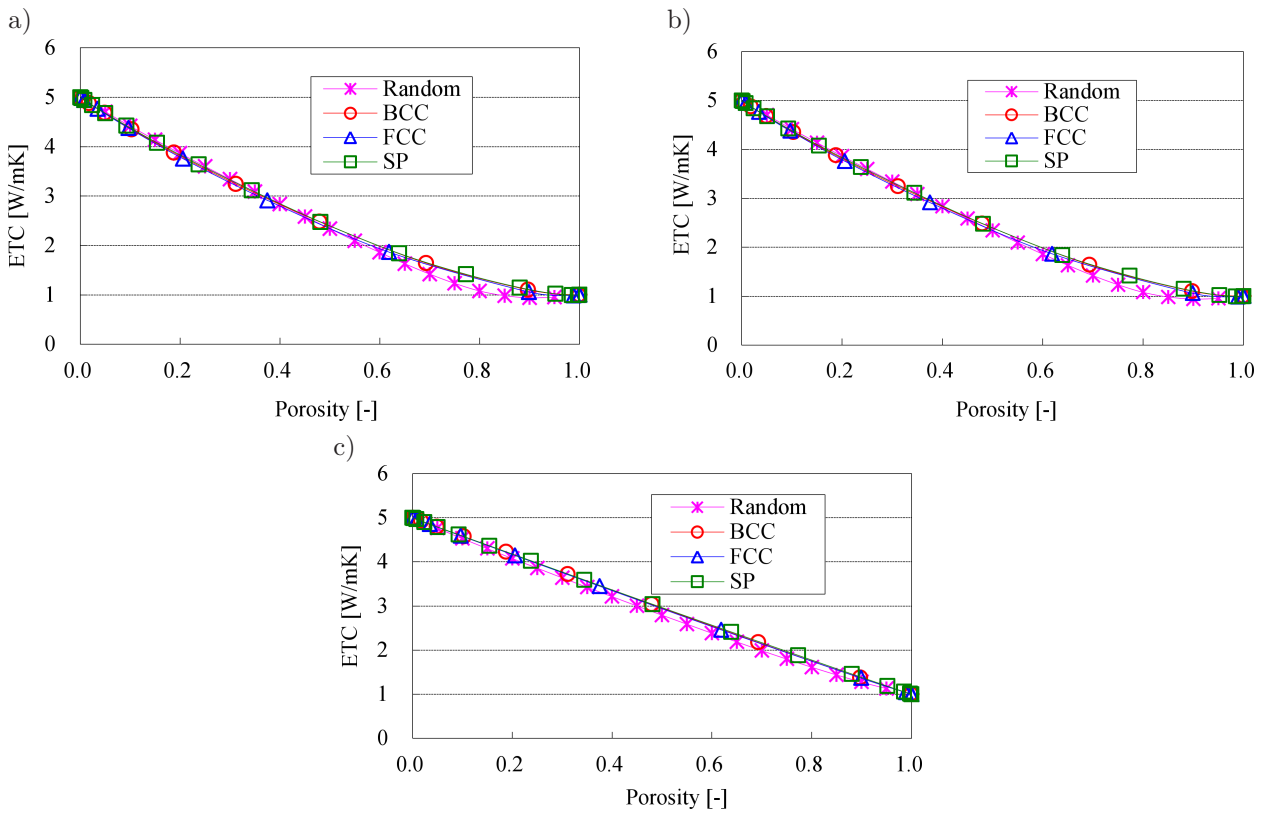


Fig. 3. ETC versus porosity for  $\lambda_s/\lambda_g = 5$ : a)  $Bi = 0.001$ , b)  $Bi = 1$ , c)  $Bi = 100$ .

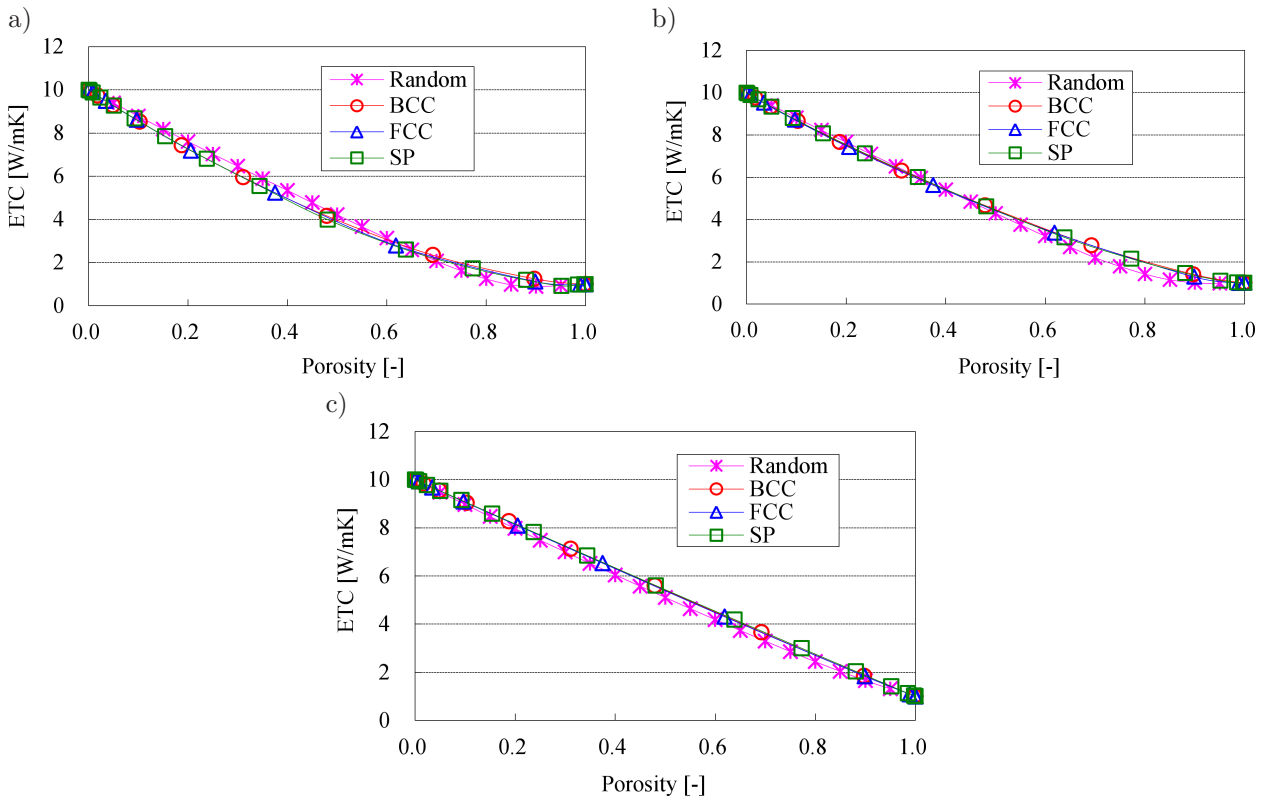


Fig. 4. ETC versus porosity for  $\lambda_s/\lambda_g = 10$ : a)  $Bi = 0.001$ , b)  $Bi = 1$ , c)  $Bi = 100$ .

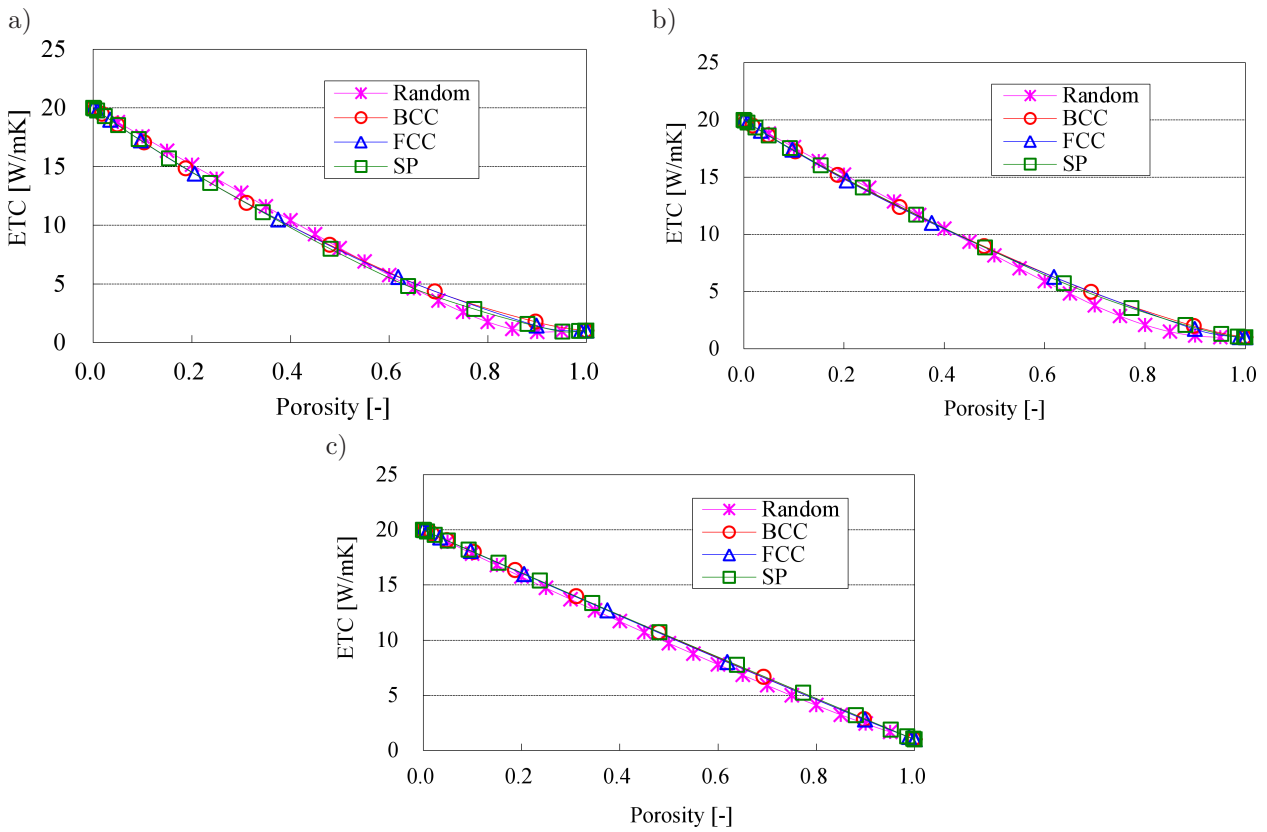
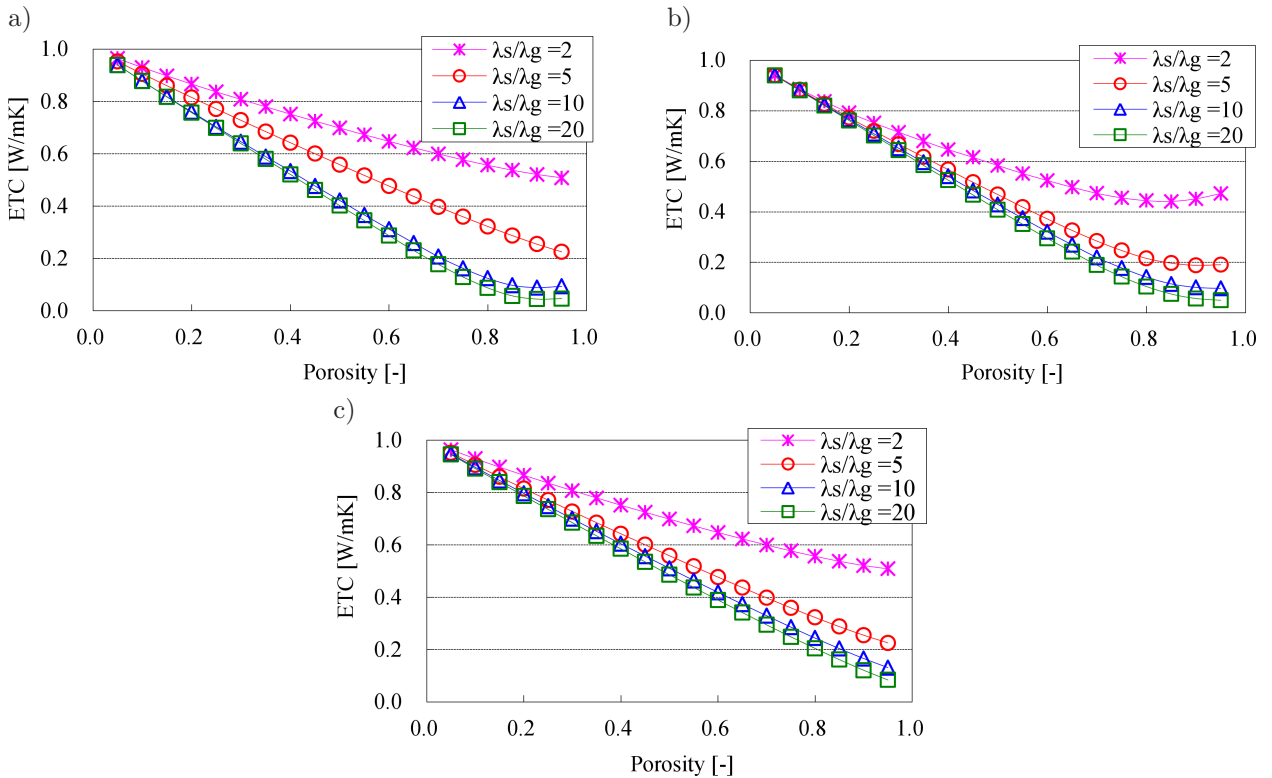


Fig. 5. ETC versus porosity for  $\lambda_s/\lambda_g = 20$ : a)  $Bi = 0.001$ , b)  $Bi = 1$ , c)  $Bi = 100$ .

(i.e., pore formation occurs). Accordingly, heat is conducted through both the solid and gas phases, and consequently minimal heat penetration occurs. The Biot number is intermediate in value in Fig. 2b and there is less heat penetration. With respect to a random phase distribution model, heat penetration through the gas phase is more difficult. Because the pathway through the gas phase in the case of a random pore distribution is at a greater porosity (0.85) than that which occurs in BCC, FCC, and SP configurations, the thermal conductivity is slightly higher. This means that pore shape and distribution are important factors for heat transfer. On the other hand, as shown in Fig. 2c, when the Biot number is greater, the thermal conductivity linearly decreases with respect to porosity. There is efficient heat transfer around the interface with respect to each porosity value.

When the thermal conductivity ratio ( $\lambda_s/\lambda_g$ ) increases, as shown in Figs. 3–5, the influence of the gas phase heat conduction becomes progressively smaller. The thermal conductivity eventually becomes linear regardless of the Biot number (Fig. 5). Porosity influences the heat conduction of a porous material via the effective conductivity. This means that when the Biot number and conductivity ratio between the gas and solid phases are smaller, the influence of the pore structure must be considered. If the pore is regularly distributed (such as in BCC, FCC, and SP configurations), the interfacial areas of the unit cells are identical. However, because the interface of a random cell (which has various pore shapes and porosities) is more extensive and the Biot number of a closed pore is smaller, one must pay careful attention to the material structure when modeling a real-life porous material (e.g., there may be a nonlinear relationship between the ETC and material porosity). Real-life ETC values should be between those of random and FCC models. In the context of overcoming this nonlinearity limitation, Fig. 6 shows normalized effective conductivity ( $\lambda_{\text{eff}}/\lambda_s$ ) values that correspond to a randomly packed model for each Biot number. We observed particle packing effects (i.e., a nonlinear relationship between the normalized effective conductivity and material porosity) with respect to only greater porosities and smaller effective conductivity ratios.



**Fig. 6.** Normalized effective conductivity ( $\lambda_{\text{eff}}/\lambda_s$ ) versus porosity for various  $\lambda_s/\lambda_g$  values: a)  $Bi = 0.001$ , b)  $Bi = 1$ , c)  $Bi = 100$ .

### 3.2. Composite

Figure 7 shows the ETC for composites (conductivity ratio  $\lambda_d/\lambda_c = 2, 5, 10,$  and  $20$ ) with respect to each particle dispersion model (BCC, FCC, SP and random). We obtained a linear relationship with respect to the particle volume ratio and conductivity for every particle packing condition. The conductivity ratio of the continuous and dispersed phases is essential for heat conduction, even for heterogeneous composites. Note that we ignored the interfacial resistance, which depends on the dispersion model, in our calculations. We did not obtain a linear relationship with respect to imperfect contacts. Results that consider interfacial resistance might be similar to those of a porous material.

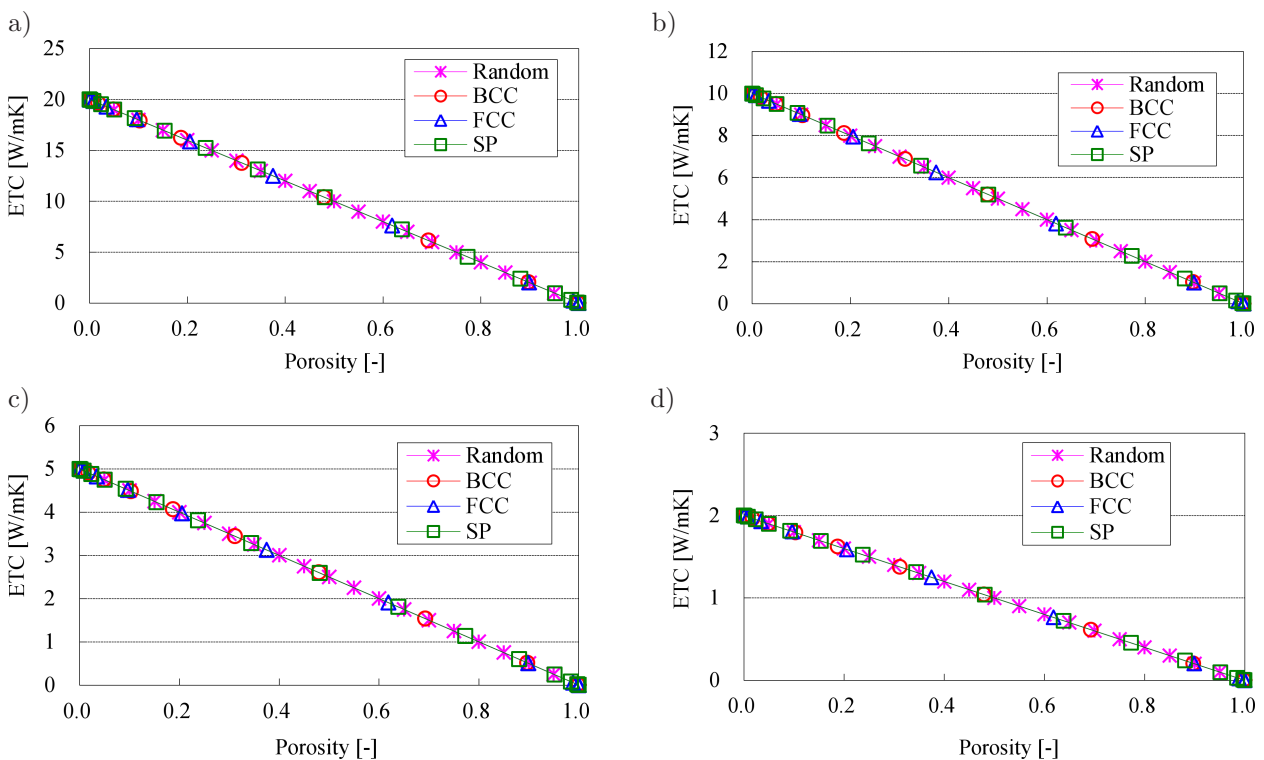


**Fig. 7.** ETC versus particle volume ratio for composite: a)  $\lambda_d/\lambda_c = 20$ , b)  $\lambda_d/\lambda_c = 10$ , c)  $\lambda_d/\lambda_c = 5$ , d)  $\lambda_d/\lambda_c = 2$ .

### 4. CONCLUSION

We have introduced homogenization as new multi-scale model for heat conduction and transfer analysis of a porous material and composite. Our method could become a powerful tool for quantitating the ETC of a material with respect to microscopic features such as particle packing, porosity and the Biot number. We have theoretically investigated the effect of pore distribution on heat transfer. Most notably, a greater porosity corresponded to a nonlinear relationship between the porosity and ETC when the thermal conductivity ratio and the Biot number were small. Both the conductivity ratio and the volumes of the continuous and dispersed phases are important parameters for heat conduction in a composite.

### REFERENCES

- [1] Y. Asakuma, S. Miyauchi, T. Yamamoto, H. Aoki, T. Miura. Homogenization method for effective thermal conductivity of metal hydride bed. *International Journal of Hydrogen Energy*, **29**: 209–216, 2004.

- 
- [2] J.L. Auriault, H.I. Ene. Macroscopic modeling of heat transfer in composites with thermal barrier. *Int. J. Heat and Mass Trans.*, **38**(18): 2885–2892, 1994.
  - [3] P.W. Chung, K.K. Tamma. Homogenization of temperature-dependent thermal conductivity in composite materials. *J. Thermophysics and Heat Transfer*, **15**(1): 10–17, 2001.
  - [4] A. Griesinger, K. Spindler, E. Hahne. Measurement and theoretical modelling of the effective thermal conductivity of zeolites. *Int. J. Heat and Mass Trans.*, **42**: 4363–4374, 1999.
  - [5] H. Hasselman, L.F. Johnson. Effective Thermal Conductivity of Composites with Interfacial Thermal Barrier Resistance. *J. Composite Materials*, **21**: 508, 1987.
  - [6] R.P.A. Rocha, M.E. Cruz. Computation of the effective conductivity of unidirectional fibrous composites with an interfacial thermal resistance. *Numerical Heat Transfer part A*, **39**: 179–203, 2001.
  - [7] H. Sun, S. Di, N. Zhang, W. Changchun. Micromechanics of composite materials using multivariable finite element method and homogenization theory. *Int. J. Solids and Structures*, **38**(17): 3007–3020, 2001.
  - [8] M.B. Taghite, A. Rohmattulla, H. Lanchon-Ducaquis, K. Taous. Homogenization of thermal problem in the plate of a heat exchanger. *Comput. Methods Appl. Mech. Eng.*, **145**: 381–402, 1997.
  - [9] K. Terada, T. Ito, N. Kikuchi. Characterization of the mechanical behaviors of solid-fluid mixture by the homogenization method. *Comput. Methods Appl. Mech. Eng.*, **153**: 223–257, 1998.
  - [10] J.L. Auriault, Heterogeneous medium, is an equivalent macroscopic description possible?, *Int. J. Eng. Sci.*, **29**: 785–795, 1991.